Tutor

Dr. Juan Carlos Paniagua Valle
Departament de Química Física

Grau de Química

Treball Final de Grau

Computational study of the CH···S interaction in a dimer to assess its eventual hydrogen bond character

Estudio computacional de la interacción CH···S en un dímero para determinar su eventual carácter de enlace de hidrógeno

Gian Pablo Fahle

June 2015

Universitat de Barcelona

Campus d'Excel·lència Internacional
BKC Barcelona Knowledge Campus

Le savant n'étudie pas la nature parce que cela est utile; il l'étudie parce qu'il prend plaisir et il y prend plaisir parce qu'elle est belle. Si la nature n'était pas belle, elle ne vaudrait pas la peine d'être connue, et la vie ne vaudrait pas la peine d'être vécue.

Henri Poincaré

And yet the concept of a chemical bond, so essential to chemistry, and with a venerable story, has a life, generating controversy and incredible interest. Even if we can't reduce it to physics, [...] push the concept to its limits, accept that a bond will be a bond by some criteria, maybe not by others, respect chemical tradition, have fun with the richness of something that cannot be defined clearly, and spare us the hype.

Roald Hoffman (Contemporary Aspects of Chemical Bonding, symposium of the American Chemical Society, September 2003)

I would like to express my gratefulness to my advisor, Juan Carlos Paniagua, who has guided me through the subtle aspects of quantum chemistry with patience and pedagogics, always treating me as his colleague and forgoing his work to support mine.

REPORT

CONTENTS

1. SUMMARY

The traditional view of H-bonding has been questioned over the past years, according to new experimental and theoretical evidence pointing to a much more general type of interaction. Recent IUPAC recommendations on H-bonding characterization highlight that a wide range of atoms and molecular fragments may be involved in H-bonding.

In this study the H-bond character of a CH···S contact between a methyl group and a sulphur atom from a thioether was assessed. These atoms come in contact in the dimerization of a trityl radical. Several criteria for identifying H-bonds were studied. These include structural-energetic, spectroscopic (IR and NMR spectroscopies) and theoretical (AIM analysis of the electron density) considerations, which were studied using a computational approach.

A medium-quality computational model was used, whose validity was assessed by first studying the mentioned interaction in the $CH_4 \cdots SH_2$ model complex and comparing the results to those reported in an analogous study by Rovira and Novoa. The chosen computational model describes well the geometries of the complex, although it fails to describe quantitatively the stabilization energy. When studying the criteria reported by the IUPAC, the chosen computational model gives a qualitatively correct description of the CH···S contact in the $CH_4 \cdots SH_2$ complex, confirming the presence of a weak H-bond, as reported in other studies.

For the CH···S contact in the trityl radical dimer a weak blue-shifting H-bond is confirmed between the indicated atoms. The interaction lays in the limit of weak H-bonding and van der Waals interactions.

Keywords: hydrogen bonding, intermolecular interactions, trityl radical dimer, density functional theory, atoms in molecules theory, computational chemistry.

2. RESUMEN

El concepto tradicional de enlace de hidrógeno ha sido cuestionado en los últimos años, de acuerdo con nuevas evidencias experimentales y teóricas que apuntan a un tipo de interacción mucho más general. Las últimas recomendaciones de la IUPAC sobre caracterización de enlaces de hidrógeno destacan el amplio abanico de átomos y fragmentos de átomos que pueden participar de un enlace de hidrógeno.

En este estudio se ha determinado el carácter de enlace de hidrógeno del contacto entre los átomos CH···S de un grupo metilo y un átomo de azufre de un tioéter. Estos átomos entran en contacto en la dimerización de un tipo de radical tritilo. Se han estudiado varios criterios para la identificación de enlaces de hidrógeno. Éstos incluyen consideraciones estructurales-energéticas, espectroscópicas (de las espectroscopias IR y RMN) y teóricas (el análisis de la densidad electrónica según la teoría AIM), las cuales se estudiarán empleando métodos computacionales.

Se ha utilizado un modelo computacional de calidad media, cuya validez se ha comprobado estudiando primero la interacción mencionada en el complejo $CH_4 \cdots SH_2$ y comparando los resultados con los obtenidos por Rovira y Novoa en un estudio análogo. El modelo computacional escogido describe bien las geometrías, aunque no proporciona energías cuantitativamente correctas. Cuando se aplican los criterios de la IUPAC a la interacción CH···S en el modelo $CH_4 \cdots SH_2$ se obtienen resultados cualitativamente correctos, los cuales confirman la presencia de un enlace de hidrógeno, tal y como sugieren otros estudios.

El estudio de la interacción CH···S en el dímero confirma la presencia de un enlace de hidrógeno débil con corrimiento hacia el azul entre los átomos indicados. La interacción se encuentra en el límite de enlaces de hidrógeno débiles e interacciones de van der Waals.

Palabras clave: enlaces de hidrógeno, interacciones intermoleculares, dímero del radical tritilo, teoría del funcional de la densidad, teoría de átomos en moléculas, química computacional.

3. INTRODUCTION

3.1. CONTEXT AND DEFINITION OF THE PROBLEM TO BE STUDIED

Dynamic nuclear polarisation (DNP) is a physical phenomenon in which the large polarization of unpaired electrons in the presence of a magnetic field is transferred to neighbouring nuclei by saturating a convenient electron paramagnetic resonance (EPR) transition [1]. DNP allows the enhancement of nuclear magnetic resonance (NMR) spectroscopy by permitting an increase of the nuclear spin polarization, transferred from the electron spin polarization by microwave irradiation [2]. The DNP enhanced NMR spectroscopy is, hence, a technique of great interest since it allows to overcome the principal limitation of NMR spectroscopy: its very low sensitivity as compared to other analytical methods. In order to perform a DNP-NMR experiment, a polarizing agent has to be present in the matrix that contains the studied molecule. This polarizing agent is a paramagnetic compound (generally organic radicals) whose electron spin polarization will be transferred to the nuclei of interest.

The University of Barcelona (UB) was one of the first universities in the world to implement DNP enhanced NMR spectroscopy. Currently, Dr. Pons' group leads the investigations in this field at the UB, with computational and theoretical assistance of Dr. Paniagua's research group. In the course of their investigations, the behaviour of some trityl radicals, used as polarizing agents in DNP-NMR (among them the Finland radical, shown in Scheme 1), at different concentrations was studied, concluding that the radicals can assemble to dimers and other supramolecular entities [3]. In an attempt to study the origin of the stabilisation energy resulting from the aggregate formation, an unusual short CH···S distance was noticed between a terminal methyl group and a sulphur atom from a cyclic thioether, suggesting the presence of a hydrogen bond between those atoms.

The purpose of this study is to evaluate the nature of the interaction between the mentioned atoms, attempting to classify it as a hydrogen bond or some other intermolecular interaction. The approach taken will be a computational one.

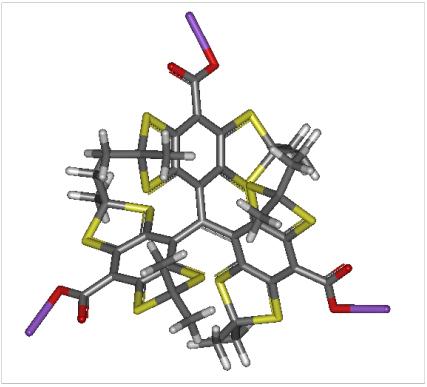

Scheme 1. Finland trityl radical. From now on referred to as *monomer*.

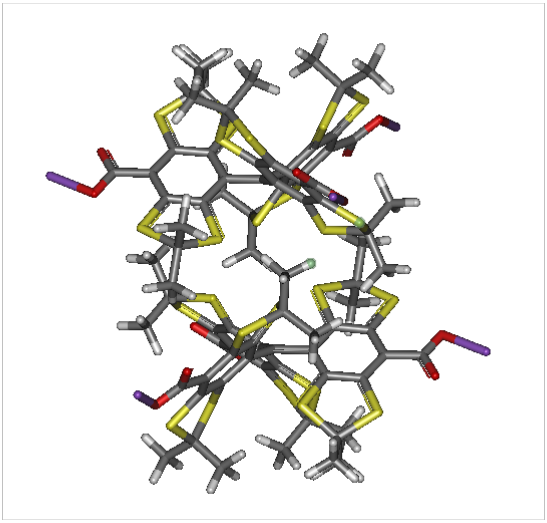

Scheme 2. The dimer to what trityl monomers assemble according to Ref. [3]. From now on referred to as *dimer*. The H and S atoms involved in the CH···S contact object of study are highlighted in green.

In this first introductory section the basic theories used in this study are reviewed. First, the hydrogen bond will be defined and a list of criteria to evaluate it will be given, based on IUPAC 2011 recommendations, which rely heavily on theoretical criteria. A review of Density Functional Theory (DFT) is given and Atoms in Molecules (AIM) theory is introduced. For both DFT and

AIM very brief reviews will be given, highlighting the basic physical concepts and focusing primarily on their practical applications. For the more interested reader, further extended descriptions of DFT and AIM theory can be found in the mentioned references.

In Section 4 the objectives of this study are defined. In Section 5 the methods used to approach the stated objectives are described; first, the specific strategies used to study weak intermolecular interactions will be mentioned, following with a schematic description of the computational models used as well as of the calculations carried out. In Section 6 the results obtained by the application of the previously mentioned methods are presented, as well as a discussion of their meaning and an attempt to give them a detailed but also general interpretation. Finally, in Section 7 the most important conclusions are highlighted.

3.2. A CONCEPTUAL REVIEW OF HYDROGEN BONDING

3.2.1. Definition and nature of hydrogen bonding

The first mention to the hydrogen bond (H-bond) in the literature is in an article by Latimer and Rodebush [4] published in 1920, where they describe that «a lonely pair of electrons of a water molecule exerts sufficient force on a hydrogen atom hold by a pair of electrons to another water molecule to consider both molecules stay united […]. A hydrogen nucleus hold between two octets constitutes a weak "bond"» (the quotation marks are by Latimer and Rodebush). Pauling made this concept popular in his book *The Nature of the Chemical Bond* published in 1939 [5], in which he defines the H-bond as an electrostatic interaction, arguing that if it were of covalent nature the involved hydrogen atom would violate the octet rule. In fact, Pauling admitted that H-bonding must have some degree of covalency. For the O-H···O contact between two water molecules Pauling estimated a degree of covalency of about 5%, based on the O-H distances in a free and a H-bonded water molecule.

The "classical" definitions to H-bonding could be reviewed with the following, in which no mention is done to the nature of the forces involved in H-bonding:

> «A H-bond is a relatively strong non-covalent interaction between a hydrogen atom covalently bonded to a very electronegative atom X (called *H-donor*) and another very electronegative atom Y (called *H-acceptor*):
>
> Y···H-X

The atoms X and Y must be atoms of fluorine, oxygen or nitrogen.»

Nowadays, although there is still no clear consensus about the nature of the forces involved in H-bonding, it is accepted that the spectrum of H-donors and H-acceptors is much broader than indicated in the previous "classical" definition. This fact is considered in the definition to H-bonding given by the IUPAC in 2011 [6]:

> «The H-bond is an attractive interaction between a hydrogen atom from a molecule or a molecular fragment X-H in which X is more electronegative than H, and an atom or a group of atoms in the same or a different molecule, in which there is evidence of bond formation.»

The definition given by the IUPAC does not specify the nature of the H-donor nor the H-acceptor groups, even accepting as a H-acceptor the π electronic system of a double or a triple bond. It has been proven [7] that any atom with greater electronegativity than hydrogen (F, N, O, C, P, S, Cl, Se, Br and I) can act as a H-donor and that any of these atoms as well as π electronic systems can act as H-acceptor. Even situations in which the H-acceptor is a hydride have been described, as well as interactions where a methyl radical acts as a H-acceptor or where methane acts as a H-donor.

Taking in mind the great variety of atoms or groups of atoms that can be involved in a hydrogen bond, it is clear that it is not an easy task to give a unique explanation to the physical nature of this interaction. Today it is well accepted [7] that H-bonding has contributions from electrostatic interactions between permanent multipoles, polarization or induction between permanent and induced multipoles; dispersion arising from instantaneous multipoles-induced multipoles; charge-transfer-induced covalency, and exchange correlation effects from short-range repulsion due to overlap of the electron distribution. There are studies that have successfully divided the total interaction energy into its components. However, this is not always possible and may not be applied to a general description of H-bonding. Clearly no single physical force can be attributed to H-bonding; either can it be classified as a type of dispersion force, since H-bonding presents a predominantly directional nature as opposed to the more isotropic nature of London dispersion forces, nor can it be described as a covalent interaction [7]. Buckingham summarizes this facts in a very elegant way writing that «The hydrogen bond results from inter-atomic forces that probably should not be divided into components, although no doubt electrostatic and overlap interactions are the principal ingredients.» [8].

3.2.2. Properties that define a hydrogen bond

Given the general and undefined nature proposed for the physical forces of H-bonding and the broad spectrum of atoms or groups of atoms that can be involved in it, the IUPAC recommends for the identification of H-bonds a series of structural, energetic, spectroscopic and theoretical criteria [6,7]. These criteria will be summarized as follows. It is highlighted that the identification of some interactions as H-bonds may be difficult and ambiguous, in which case the characterization of the interaction as a H-bond will be more reliable as more criteria are met. Both experimental and theoretical methods are accepted, although a combination of them is recommended.

3.2.2.1. Distance and energy criteria

The comparison of bonding distances between systems exhibiting H-bonds and systems without H-bonds has been a "classical" criterion for the identification of H-bonds. Nowadays, however, the use of this criterion is discouraged.

A classification of H-bonding based on the interaction energy is proposed, into strong H-bonds (63-167 kJ mol^{-1}), medium (17-63 kJ mol^{-1}) and weak (<17 kJ mol^{-1}), with notably no lower limit for weak H-bonds. Moreover, a relationship between the intensity of the interaction energy of a H-bond and the nature of the involved forces is proposed, stating that the electrostatic contribution is greater as higher the energy is, whereas the contribution of dispersion forces is greater as weaker the interaction is.

However, although energy criteria may be very useful for identifying a H-bond, the IUPAC recommends as ultimate structural-energetic criteria the directionality of H-bonding. The dependence of the interaction energy with some bonding direction allows distinguishing between a weak H-bond and a dispersion force, of isotropic nature.

3.2.2.2. Spectroscopic criteria

Spectroscopic evidences have been, and still are, considered the most sensitive and characteristic criteria for identifying the formation of a H-bond. Specially, changes in the stretching frequency associated to the X-H bond in an IR spectrum are considered fundamental characteristics to identify H-bond formation. Until the end of the 20th century all the types of H-bonds studied presented a red-shift in their X-H stretching frequency upon H-bond formation. Nonetheless, nowadays it is known that there are H-bonds that present blue-shifts or even no

shift in their stretching frequencies. Joseph and Jemmis [9] provide a unified explanation for red-, blue and no-shift of X-H stretching frequencies upon H-bond formation. Iogansen [10] showed that there is a strong correlation between the H-bond strength and the intensification of the X-H band associated to H-bond formation.

NMR spectroscopy offers the next best evidence for H-bonding after IR spectroscopy. In general, the proton magnetic resonance of XH moves toward a lower field compared to non-H-bonded XH due to a strong deshielding of the protons. Moreover, NMR spectroscopy has provided direct evidence for through-bond coupling between X and Y in a X-H···Y H-bonded system. Also, in complexes containing a quadrupolar nucleus the nuclear quadrupole coupling constants (NQCC) can change due to the distortion of electronic environment around these atoms, following H-bond formation.

Besides the evidences offered by IR and NMR spectroscopies, which the IUPAC puts more emphasis on and which will be the ones considered in this study, there are several other techniques that provide useful information. Examples are electronic spectroscopy, Raman spectroscopy, vibrational circular dichroism spectroscopy or double resonance techniques (2D-IR, IR-UV, 2D-UV, 2D-RMN).

3.2.2.3. Theoretical criteria

When talking about “theoretical criteria” or “computational methods” it is important to make a distinction that may not be evident in this context. The structural, energetic and spectroscopic criteria mentioned above may be evaluated by means of experimental or computational methods. The fact of studying one of these criteria using a computational method does not convert it in a theoretical criterion; it stays a structural-energetic or spectroscopic criterion, which is studied using a computational approach. On the other hand, there are criteria that allow to identify H-bonds which are inaccessible for an experimental approach; not because of a great difficulty or unviability of an experimental study but because there are no experimental methods available for the study of that property. Those are the so-called theoretical criteria, which can only be studied by a computational approach. The IUPAC offers in its paper recommendations for both the use of computational methods –indistinctly of what criterion is evaluated– as well as for pure theoretical criteria.

When talking about computational methods, the IUPAC discourages the use of methods other than *ab initio* methods or methods based on the density functional theory (DFT). For both

methods it is recommended to always consider the basis set superposition error if the supermolecule approach is used for the energy evaluation. For DFT methods, the need for including functionals that consider dispersion forces is highlighted.

As theoretical criteria inaccessible from experiment, the information obtained from a natural bond order (NBO) analysis or from an atoms in molecules (AIM) analysis is highlighted. The use of AIM theory for studying a H-bond is highly recommended and the detection of a (3,-1) critical point (a bond critical point) is explicitly mentioned as a criterion for identifying a H-bond.

3.3. DENSITY FUNCTIONAL THEORY

3.3.1. Density functional theory: Hohenberg-Kohn theorems

Density functional theory is a quantum theory of electronic structure of matter that aims to obtain information of a physical system from its electron density rather than from its corresponding wave function. Hohenberg and Kohn established the basic theoretical framework of DFT in 1964 and Kohn and Sham proposed a practical implementation in 1965.

The DFT theoretical framework is based on two theorems: the existence theorem and the variational principle. The existence theorem establishes the electron density as the basic variable for describing and determining the ground-state properties, particularly the total energy, of a system of interacting particles [11]. The existence theorem states that *the ground-state density* $\rho(\vec{r})$ *of a bound system of interacting electrons in some external potential* $v(\vec{r})$ *determines this potential uniquely* [12,13]. A few remarks have to be added: (i) The term "uniquely" means here: up to an uninteresting additive constant. (ii) In the case of a degenerate ground-level, the lemma refers to the density of any of its degenerate states. (iii) This lemma is mathematically rigorous.

The "external potential" to which Hohenberg and Kohn refer is, in the simplest case, the potential that arises from the positive charges of the nuclei (the attractive electron-nuclei potential), but can also be some other potential to which the molecular system is exposed. Since the potential fixes the Hamiltonian of the system, a theorem establishing a unique relation between the potential and the electron density leads to the full many-particle ground state being a unique functional of the electron density. Hence the electron density also determines implicitly all properties derivable from the Hamiltonian through the solution of the Schrödinger equation.

The second theorem of Hohenberg and Kohn, the variational principle, establishes the basis for the practical implementation of the first theorem. The variational principle states a minimal principle for the ground-state energy in terms of the electron density:

$$E = \min_{\tilde{\rho}(\vec{r})} E_v[\tilde{\rho}(\vec{r})] = \min_{\tilde{\rho}(\vec{r})} \left(\min_{\alpha} \langle \tilde{\Psi}^{\alpha}_{\tilde{\rho}} | \hat{H} \tilde{\Psi}^{\alpha}_{\tilde{\rho}} \rangle \right) \qquad (1)$$

where $\tilde{\rho}(\vec{r})$ is a trial density and $\tilde{\Psi}^{\alpha}_{\tilde{\rho}}$ the class of trial functions with this density; E is the total energy of the system, $E_v[\tilde{\rho}(\vec{r})]$ the constrained energy minimum and $\hat{H}$ the Hamiltonian describing the system's energetics.

Hence, Hohenberg and Kohn state an exact theory that establishes the electron density as the basic variable for describing the ground-state properties of an interacting particles system and they give the basis for a practical implementation for the search and calculation of those properties in terms of the electron density.

3.3.2. Practical implementation of DFT: the Kohn-Sham method

In 1965 Kohn and Sham established a practical implementation of DFT by proposing the Kohn-Sham (KS) method, a set of self-consistent equations that, if resolved iteratively, should lead to the ground-state electron density and energy of an interacting particles system [13,14].

Although DFT, in terms of the HK formulation, establishes a direct relationship between the ground-state properties and the electron density (independently of the wave function), this direct relationship is still inexplorable in practical terms. There is no way for determining the electron density of an interacting particles system other than the experimental determination or the previous calculation of the wave function. So, when implementing DFT, the usual way for obtaining the electron density is through the previous determination of the corresponding wave function, from which the electron density is then calculated.

The KS self-consistent equations and the Hartree-Fock (HF) self-consistent equations are essentially analogous, only differing in the mathematical expression of the potential energy of the monoelectronic Hamiltonian operator.

In an HF context the correlation energy is defined as the difference between the HF-limit energy (that is, the energy calculated on a HF level using a high-quality basis set) and the exact energy. To account for that energy after a HF calculation multireferential methods must be used, such as the configuration interaction (CI) method. These methods have a great associated computational cost.

The KS approach, on the other hand, explicitly introduces an exchange correlation functional in the expression for the total energy. Although the exact form of this functional is still unknown, accurate approximations to it have been made. The introduction of this exchange correlation functional in the expression of the total energy does not imply a significant extra computational cost. This last fact is the feature that makes the KS method a much more useful and promising approach than the HF method. The latter has already reached a "top", meaning that improvements on the HF method –understanding "improvements" as efficiency improvements– can only be achieved by developing better basis set functions or more efficient calculation algorithms. On the other hand, DFT is still open to "theoretical" improvements, that is, a better understanding of DFT may lead to the establishment of equations that only depend on the electron density without the need of the wave function. If this is ever achieved, DFT could become an even more powerful tool for theoretical chemistry.

For the mathematical details of the HK theorems and the KS method, as well as a more rigorous and extended description, the reader should refer to Refs. [11,13].

3.3.3. Consideration of exchange correlation in the Kohn-Sham method

In the KS formulation of DFT the kinetic energy, the electrostatic electron-electron repulsion and the electron-nuclei attraction are obtained by considering every electron independent from the rest. All the energetic contributions that cannot be described by an independent electron model are included in the exchange correlation functional [13]. If this functional were known, the KS-DFT formalism would be exact and would lead to the exact energy (except for some specific cases in which the electron density cannot be obtained from a monodeterminantal wave function).

However, the exchange correlation functional is still unknown and approximations must be introduced. Several attempts have been made to obtain as accurate as possible approximations to the exchange correlation functional. Many of them include empirical parameters. As a first general classification, the approximations can be distinguished as "pure functionals" or "hybrid functionals". Pure functionals are those that consider exchange correlation introducing an average exchange correlation potential, and hybrid functionals are those that combine expressions from pure functionals and expressions from other methods, such as HF. The combination coefficients can be obtained by theoretical considerations or optimized using empirical data.

3.3.4. Consideration of dispersion forces in the Kohn-Sham method

Dispersion forces are due to long-range electron correlations, in which an attractive interaction appears originating from the response of electrons in one region to instantaneous charge density fluctuations in another. Standard exchange correlation functionals do not describe this correlation because of two reasons: (i) instantaneous density fluctuations are not considered; and (ii) they are "short-sighted" in that only local properties are considered for calculating the exchange correlation energy [15,16].

Dispersion forces can contribute significantly to the binding of many supramolecular aggregates, as well as to the preferred conformation of a given molecular system. In order to describe correctly the energetics of such systems, DFT methods must include corrections that consider dispersion forces. Many approaches to treat dispersion forces have been suggested [16]. The simplest ones just include a term that considers the $1/r^6$ decay of the dispersion interaction, adjusted to each type of element via fixed empirical coefficients. More sophisticated corrections optimize these empirical coefficients according to each atom's environment and its polarizability. Even more accurate approaches include non-local (i.e., long-range) correlations to local or semi-local correlation functionals. Obviously, the more sophisticated the corrections are, the higher is the associated computational cost.

3.4. ATOMS IN MOLECULES THEORY

3.4.1. Objectives and methodologies of Atoms in Molecules theory

The theory of atoms in molecules (AIM theory, sometimes also called QTAIM, from quantum theory of atoms in molecules) suggests obtaining information about the atoms, bonding and structure that define a molecular system from its electron density or, more precisely, from the topology of that electron density [17-19]. The basic idea behind AIM theory is that the conceptual basis of chemistry is a consequence of structure that is evident in real space, and that empirical concepts such as functional groups or other basic concepts in chemistry such as atoms and bonds in a molecular system should be possible to define in a quantum language.

So, AIM theory proceeds by first calculating the electron density of a given molecule and then analysing its topological features. Each of these topological features can be associated to a chemical concept –an atom in a molecule or a bond, for example– and allow for describing and interpreting it using the quantum formalism. AIM theory tries to unify theoretical chemistry

and more empirical branches of chemistry that rely on concepts such as Lewis structures, electronegativities or functional groups, for example.

In this section only a basic description of the most fundamental concepts of AIM theory will be given, with the attempt to familiarise the reader with concepts that will be used in further sections. The more interested reader should refer to Refs. [17,18].

3.4.2. Analysis of the topology of the electron density

Each topological feature of the electron density $\rho(\vec{r})$, whether it be a maximum, a minimum or a saddle point has associated with it a *critical point* (abbreviated to cp) denoted by the coordinate $\vec{r}_c$, where $\nabla\rho(\vec{r}_c) = 0$. These cps can be classified attending to certain characteristics of the hessian matrix of ρ evaluated at the cp.

There are four types of cps that can be found in the analysis of the electron density. Each one of them allows identifying, respectively, an atomic nucleus, the centre of a chemical bond, the centre of a set of atoms forming a ring and the centre of a set of atoms forming a cage. Further analysis of the electron density permits the definition of an atom or the identification of bonded atoms. These identifications are based on the analysis of gradient paths, which are curves in space that follow the direction of steepest ascent in ρ.

An atomic nucleus is defined at the coordinates of a cp where the electron density is a maximum. An atom in a molecule is defined by the surface that encloses an atomic nucleus and which is not crossed by any gradient path line. A chemical bond is identified when an accumulation of electron density is observed between two nuclei. When viewed in one certain unique line connecting the two nuclei, the electron density exhibits a minimum at the bond cp; when viewed from any other direction, the electron density is a maximum at the bond cp. Thus, the electron density presents the topology of an “inverted saddle point” when there is bonding between two atoms.

3.4.3. AIM perspective of hydrogen bonding

The topological features of the electron density at a cp of a hydrogen bond (H-bond) can be used as criteria for quantifying the H-bonding interaction [20,21]. Both the electron density and its hessian evaluated at the cp are parameters that are linearly related to the stabilization energy of the H-bond, i.e. with H-bond strength. It is remarkable that the energy of interaction is governed only by one parameter –the electron density at the cp– over the whole range of

interaction energies, from the very weak (van der Waals) level up to that of strong H-bonds. This approach is the opposite of the usual description of H-bonds as a sum of different components – electrostatic, polarization, delocalization, charge-transfer– whose relative contributions vary widely, so the cannot be used to individually represent the whole range of interaction energies.

Besides the theoretical approach of AIM theory, a direct proportionality was suggested between the H-bond energy and the intensification of the IR stretching mode of the H-bond donor group on H-complex formation [10].

4. OBJECTIVES

The main purpose of this study is the evaluation of the CH···S interaction present in the dimer, in order to assess its H-bond character. For achieving this objective, the recommendations on H-bonds given by the IUPAC [7] will be followed. These include:

- Evaluation of the energy and the directionality of the interaction.
- Calculation of IR frequencies and intensities.
- Calculation of NMR parameters: chemical shifts, spin-spin scalar coupling constants (SSCC) between the H-acceptor and the H-donor and nuclear quadrupole coupling constants (NQCC).
- AIM based analysis of the electron density.

Besides these criteria, other relationships will be explored, namely the correlation of the H-bond strength to specific parameters: the electron density at the H-bond cp and the intensity of the spin-spin coupling between the H atom and the H-donor.

The stated criteria will be studied following a computational approach. Considering the size of the dimer, a medium-quality computational model will be used. In order to determine its validity, the criteria will first be applied to study the CH···S interaction between methane and hydrogen sulphide. The results will be compared to an analogous study by Rovira and Novoa [38]. Thereafter, different approaches for evaluating non-covalent interactions will be applied to the dimer, in order to study the H-bond character of the CH···S contact by applying IUPAC's recommendations.

5. COMPUTATIONAL ASPECTS

5.1. STRATEGIES AND APPROACHES FOR EVALUATING WEAK INTERACTIONS

5.1.1. The supermolecule approach

The most widely used method for determining the interaction energy of a molecular cluster formed by monomers held by intermolecular forces is the so-called supermolecule approach [22]. This approach evaluates the stabilization energy ΔE of a molecular cluster $\mathrm{R}\cdots\mathrm{T}$ formed from subsystems R and T following eq. 2:

$$\Delta E = |E(\mathrm{R}\cdots\mathrm{T})| - |E(\mathrm{R}) + E(\mathrm{T})| \qquad (2)$$

where $E(\mathrm{R}\cdots\mathrm{T})$, $E(\mathrm{R})$ and $E(\mathrm{T})$ denote the total energies of the molecular cluster $\mathrm{R}\cdots\mathrm{T}$ and the subsystems R and T (note that, being defined this way, a positive value for ΔE is an actual stabilisation whereas a negative value for ΔE is a destabilisation).

There are several advantages of the variational-based supermolecule approach (e.g., easy applicability, high accuracy or implicit inclusion of important phenomena such as many-body interactions and charge-transfer effects), but also an important drawback: the basis set inconsistency, which leads to the basis set superposition error (BSSE). The BSSE arises from the fact that in the dimer energy calculations the individual monomer takes advantage of the basis set of the whole cluster rather than of just "its own" basis set centred at this monomer [22]. As a consequence, the quality of the basis set is higher in the cluster calculation than in the separated monomer calculations, leading to overestimates of the stabilization energy when evaluated by the supermolecule approach. The typical values of the BSSE are of the same magnitude than the stabilisation energy of complexes hold by non-covalent interactions, so the BSSE must always be considered. The BSSE, which is a purely mathematical artefact, can be eliminated by the counterpoise (CP) method suggested by Boys and Bernardi [23]. Also, if extended basis sets are used, the BSSE converges to zero. The convergence is, however, very slow, and the use of extended basis sets is not viable for large molecular clusters. In a very rough description, the CP method suggested by Boys and Bernardi eliminates the BSSE by calculating the monomer energies to be used in eq. 2 with the full cluster basis. Some objections have been made to the Boys and Bernardi CP method and other CP methods have been developed, although the basic idea on which they rely is the same for all of them.

5.1.2. Other approaches for evaluating weak interactions

The supermolecule method is not always applicable. For example, the apparently simple and straightforward eq. 2, when applied to weak intermolecular interactions, requires subtraction of energies that are several orders of magnitude larger than the interaction energy. In many cases it is impossible to obtain $E(\mathrm{R}\cdots\mathrm{T})$, $E(\mathrm{R})$ and $E(\mathrm{T})$ with an error smaller than ΔE. On the other hand, the supermolecule approach does not allow the evaluation of a single interaction present in some cluster with a large number of non-covalent contacts that contribute each of them to the total stabilisation energy ΔE. Also, it is not possible to evaluate intramolecular non-covalent contacts by means of the supermolecule approach.

In this study, the large number of interactions present in the dimer makes it difficult to evaluate the interaction of a single CH···S contact by a supermolecule approach. In the following subsections other methods for evaluating non-covalent interactions, which are used in this study, are described.

5.1.2.1. Reproduction of interactions in simplified molecular models

One approach used in this study is the evaluation of the interaction of interest in a simplified molecular model, which is so designed that it reproduces the mentioned interaction. By using simplified molecular models two important handicaps can be solved: (i) the size of the molecular model is smaller and, therefore, the associated computational cost is much lower and higher-quality computational models may be applied, and (ii) by choosing a correct molecular model, that is, one in which presumably only the interaction of interest occurs, the supermolecule approach may be applicable.

Molecular models are fragments of the molecular cluster in which only the interacting moieties are present. These are obtained by eliminating the whole structure of the molecular cluster that does not explicitly contribute to the studied interaction. There is not a predefined methodology for determining what parts of the molecular cluster should be conserved in the model and which ones can be obviated. Molecular models must be designed using “chemical intuition” and evaluating if they correctly describe the interaction present in the molecular cluster by energy analysis.

5.1.2.2. Energy evaluations via rotation barriers

Buemi [24] suggests an alternative approach for evaluating noncovalent interactions when the supermolecule approach is not applicable; for example, for intramolecular non-covalent interactions or for evaluating a single interaction in a molecular cluster with a large number of interactions. Buemi proposes obtaining estimates to the interaction energy analysing the energy barrier associated to the rotation of the interacting atom or group of atoms, assuming that the rotation barrier is given by:

$$RB = E_{int} + RB_{free} \qquad (3)$$

where RB is the rotation barrier with the interaction, E_{int} is the interaction energy and RB_{free} is the rotation barrier without the interaction. The latter can be obtained from some other compound structurally close to the examined one but interaction free.

5.1.2.3. Energy correlations to specific properties and parameters

When trying to quantify the H-bond strength, it is usually described as the sum of different components –electrostatic, polarization, delocalization and charge-transfer– whose contribution varies as the energy of interaction does. Although it gives insight into the nature of the physical forces involved in the H-bond, it is a highly challenging approach for two reasons: (i) the determination of the extension of contribution of each of the components may be difficult, and (ii) it is not possible to correlate energy variations with a single parameter, so comparative studies are not easy.

However, certain parameters have been described that are linearly related to the stabilisation energy of the H-bond. Iogansen [10] described how the H-bond strength is correlated with the intensification of the X-H band in IR spectroscopy. Also, it has been described how the H-bond strength is linearly related to the electron density at the bond cp associated to the H-bond, as well as to its laplacian evaluated at the same point [20,21] (see Scheme 3). Rozenberg established a general relationship between the electron density at the bond cp and its corresponding stabilisation energy (standard deviations are shown in parentheses) [20]:

$$E(\text{kJ mol}^{-1}) = -6{,}6(8{,}0) + 1250(440)\rho(\vec{r}_c)\ (\text{e a}^{-3}) \qquad (4)$$

where $\rho(\vec{r}_c)$ is the electron density at the bond cp.

Also, it has been pointed out that H-bond strength correlates with changes in the intensity of the spin-spin coupling between the H-donor and the H atom itself [25]. The ^1J(XH) coupling constants are very sensitive to H-bond formation and the magnitude of their increase (in terms of a reduced coupling constant) correlates with the strength of the H-bond.

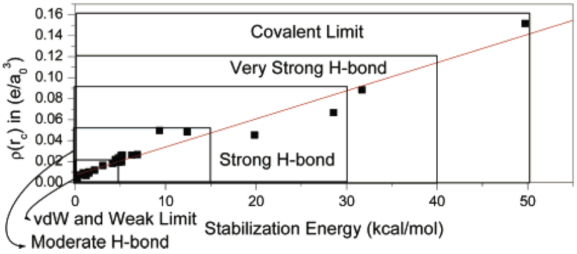

Scheme 3. Diagram showing the relationship between the electron density at the H-bond critical point and the stabilization energy for different H-bonded complexes (reproduced from Ref. [21]).

5.2. THEORIES USED IN THE CALCULATIONS

5.2.1. Computational models and computational software

All the calculations performed in this study were done using the KS-DFT method. For calculations involving the dimer or its monomers (with spin multiplicity 3 and 2, respectively) the unrestricted KS (UKS) equations were used, as well as the restricted open-shell KS (ROKS) in order to perform the AIM analyses (since the AIM software only accepts restricted wave functions). For the molecular models with no unpaired electrons the restricted KS (RKS) equations were used.

The Becke-Perdew ’86 (BP86) exchange correlation functional [26] was used, a GGA type functional that uses Becke’s 88’ exchange and Perdew’s 86’ correlation functionals. Although more efficient exchange correlation functionals exist (such as the B3LYP functional), the BP86 functional was chosen because it provides good geometries with a lower computational cost.

In order to include dispersion forces, the atom-pairwise dispersion correction with the Becke-Johnson damping scheme (D3BJ) method developed by Grimme and coworkers was used [27]. The D3BJ method considers dispersion forces with a parameterised function that describes the r^{-6} behaviour of the corresponding potential, which is optimized with empirical parameters introduced for each type of atom and its environment.

The BSSE was considered using Grimme's version of the CP method [28], known as the geometrical counterpoise (gCP) method. The gCP method, instead of determining the BSSE by obtaining the energies of the monomers using the basis set of the cluster, introduces the BSSE in a semi-empirical way. By the definition of an atom pairwise potential, the gCP gives good estimates to the BSSE with almost no computational cost. Contrary to the standard CP strategy, the gCP method can be applied to compute inter- as well as intramolecular interactions.

Calculations weren't performed considering the molecules in vacuum but in a solvent. For modelling the solvent, a polarizable continuum model (PCM) was used, the COSMO solvation model [29]. A PCM does not consider the solvent explicitly but rather as a dielectric medium outside some surface at the solute-solvent boundary. The conditions of a 1:1 mixture of water and dimethyl sulfoxide were reproduced by setting a relative permittivity of $\varepsilon_r = 53$ and a refractive index of $n = 1{,}4$.

All calculations were performed using version 3.0.3 of Neese's *ab initio*, DFT and semiempirical SCF-MO package ORCA [30], except the calculations of NMR chemical shifts and spin-spin coupling constants, which where performed using version 09 of the Gaussian computational package [31]. Gabedit 2.4.8 [32] was used as a graphical interface for visualizing and building molecular geometries, obtaining the corresponding geometry files as well as generating IR spectra and other plots. Gabedit was also used for assigning calculated IR frequencies. The AIMAll package [33] was used in order to perform AIM analyses.

5.2.2. Basis set functions

Three different basis set functions were used: the def2-SVP and def2-TZVP basis sets from Ahlrichs' group [34] and the IGLO2 basis set [35]. The def2-SVP and def2-TZVP basis set functions, split-valence and triple zeta quality functions, respectively, were used for all calculations but NMR calculations. Both basis set functions are splitted in the valence region, thus describing with higher quality the outer electrons. Also, both basis set functions include polarisation functions, which give them a higher flexibility to describe slight changes in electronic structure, a very important feature when describing non-covalent interactions [36].

Basis set functions with a higher quality describing outer electrons are important when describing properties that are mostly dependent on the valence electrons. However, when calculating NMR parameters, a higher quality for describing the inner electrons is required,

since they exhibit a major influence on the nuclear properties. The IGLO2 basis set functions, specifically developed for NMR calculations, are splitted in the core region of the atom, thus offering a higher quality when describing the inner electron distribution.

5.3. COMMON CALCULATIONS AND THEIR FOUNDATION

5.3.1. Potential energy surface explorations

All the calculations performed in this study can be viewed as having two general stages. The first stage is the potential energy surface (PES) exploration, in which the equilibrium geometries or PES minima of the studied molecular system are determined. The second stage encompasses all the properties determinations, that is, the calculations and analyses of characteristic properties.

PES explorations start with the definition of a non-optimized geometry for the molecular system of interest. This geometry is then optimized, i.e., its equilibrium geometries are searched using a geometry optimization algorithm. Geometry optimization algorithms do not necessarily converge to the absolute minimum of a PES, that is, equilibrium geometries other than the absolute minimal energy equilibrium geometry can be located. No methods exist that confirm whether a located minimum is an absolute or a relative one, so this must be solved using "chemical intuition". This is usually done by modifying certain geometrical parameters, reoptimizing the resulting geometry and comparing its optimized energy to the one of the previously obtained geometry. Generally, the PES of a molecular cluster hold by intermolecular interactions is very rich and contains a large number of energy minima.

Once an equilibrium geometry is located using a geometry optimization algorithm, its minimum nature should be confirmed. This is especially important in the search for minima in the PES of a molecular cluster, where energy minima usually are not well defined and the searching algorithm easily can get stuck. The minimum nature of a presumed equilibrium geometry can be confirmed by a frequencies calculation (also called a normal mode of vibration determination). A positive-frequency normal mode is a motion of the molecular nuclei upwards the PES; thus, it represents a vibration and will not modify the molecular conformation, since the distortion it implies leads to a more energetic point in the PES. On the other hand, an imaginary-frequency normal mode (corresponding to a negative hessian eigenvalue) reveals a tendency of the molecule to adopt a geometry that lays in a lower point in the PES, that is, a more stable

conformation. Therefore, by analysing the frequencies of a presumed equilibrium geometry, one can confirm its minimum nature: all its frequencies should be positive.

5.3.2. Calculation of properties: NMR parameters

All energetic, structural and geometric properties of interest for studying weak interactions are obtained in a geometry optimization and a subsequent normal mode calculation. The NMR parameters (chemical shifts, spin-spin coupling constants (SSCC) and nuclear quadrupole coupling constants (NQCC)) require an additional calculation with the appropriate basis.

Chemical shifts calculations require obtaining the shielding constant for the relevant nuclei. Coupling constants, on the other hand, are obtained as derivatives from the total energy respect to the nuclear magnetic moments [37].

6. RESULTS AND DISCUSSION

Four different molecular clusters containing (or presumably containing) a CH···S contact were studied. First, the methane-hydrogen sulphide complex was studied, in order to assess the adequacy of the proposed approaches for evaluating noncovalent interactions and, specifically, non-conventional H-bonds. The obtained results are compared to Rovira and Novoa's results on an analogous study [38], which suggested the existence of a H-bond between methane and hydrogen sulphide. Second, two molecular models were studied, designed to reproduce the CH···S contact observed in the dimer with simplified molecular structures. Finally, the CH···S interaction in the dimer was studied. In the following subsections the results of these calculations and an interpretation to them are given.

6.1. EVALUATION OF THE CH···S INTERACTION BETWEEN METHANE AND HYDROGEN SULPHIDE. VALIDATION OF THE COMPUTATIONAL MODELS

6.1.1. Potential energy surface minima

Following a study by Rovira and Novoa [38], the optimum geometry as well as the interaction energy of the methane-hydrogen sulphide complex was calculated. The geometry

optimizations were carried out at the RKS-DFT/def2-TZVP level, while those of Ref. [38] were performed at the MP2/6-31++G(2d,2p) level.

This complex shows two energy minima, whose structures are shown in Scheme 4. The obtained structural parameters and stabilization energies, calculated following eq. 2, are shown in Tables 1 and 2, respectively, as well as a comparison with the values from Ref. [38].

System	Parameter	Value	
		Calculated	Ref. [38]
$CH_4 \cdots SH_2$ (**c1**)	S2-H1 = S2-H3	1,35	1,34
	C4-H5 = C4-(H6,H7,H8)	1,10	1,09
	S2···H5	3,16	3,26
	<H1S2H3	92,69	92,44
	<H5C4H6	109,46	109,34
	<C4H5S2	172,45	171,31
	<H5S2H1	77,50	122,59
$CH_4 \cdots SH_2$ (**c3**)	S2-H1 = S2-H3	1,37	1,34
	C4-H5 = C4-(H6,H7,H8)	1,11	1,09
	S2···H5	3,37	3,37
	S2···H7	3,38	3,37
	C4···H1	3,71	3,17
	<H1S2H3	92,23	92,44
	<H5C4H6	109,41	109,23
H_2S	S-H	1,35	1,34
	<HSH	92,64	92,25
CH_4	C-H	1,10	1,09
	<HCH	109,47	109,47

Table 1. Some structural parameters of the conformers of the methane-hydrogen sulphide complex, comparing calculated values to those given in Ref. [38] (distances in Å and angles in degrees).

Conformer	Stabilisation energy / kcal·mol^{-1}	
	Calculated	Ref. [38]
c1	0,23	0,42
c3	0,41	0,84

Table 2. Calculated stabilisation energies of the two conformers of the methane-hydrogen sulphide complex, compared to those given in Ref. [38].

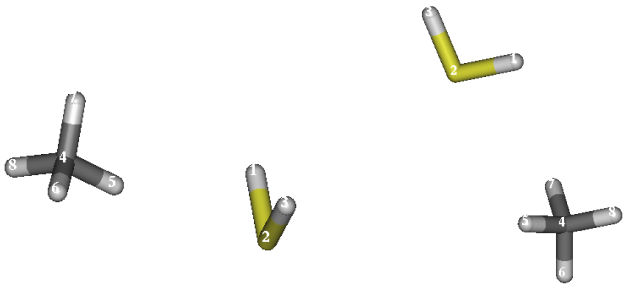

Scheme 4. Equilibrium geometries of the methane-hydrogen sulphide complex conformers optimized at the RKS-DFT/def2-TZVP level (**c1** left, **c3** right).

As can be seen in Table 1, good approximations to the equilibrium geometries for conformers **c1** and **c3** were found as comparing to Rovira and Novoa's results. Only one angle in **c1**, the <H5S2H1 angle, differs notably from the referenced values. However, the orientation of the atoms defined by that angle is not involved in the intermolecular interactions we are interested in.

On the other hand, the computational model used in this study correctly predicts the stability of both clusters, although it fails to quantitatively reproduce their interaction energies, as can be seen in Table 2. This discrepancy is probably mainly due to the lack of diffuse functions in our basis sets. Although it is known that these kinds of functions are necessary for a good description of non-covalent interactions, they have been omitted because of the great increase in the computational cost they produce in large molecular systems. Nonetheless, the obtained geometries are in good agreement to those given in Ref. [38], and, as will be shown in the next subsection, the calculated properties confirm those interactions established by the authors.

6.1.2. Calculation of properties

6.1.2.1. Distance and energy criteria

No changes are observed between the C-H and S-H bond lengths in free and clustered methane and hydrogen sulphide, respectively. This can be attributed to the very weak nature of the CH···S interaction in this complex.

6.1.2.2. Spectroscopic criteria

Both IR spectroscopy and NMR spectroscopy properties were calculated for free and clustered methane and hydrogen sulphide in order to assess the CH···S interaction. Table 3 shows the IR parameters obtained from the corresponding frequency calculations.

Bond vibration (system)	IR spectroscopy parameters: stretching frequencies / cm^{-1} (intensity / $km \cdot mol^{-1}$)	
	Calculated	Ref. [38]
C-H stretching (CH_4)	3057 (33) 3058 (38)	3218 (19)
C-H stretching ($CH_4 \cdots SH_2$ **c1**)	3055 (25) 3056 (31) 3059 (32)	3213 (20) 3213 (20) 3220 (10)
C-H stretching ($CH_4 \cdots SH_2$ **c3**)	3050 (9) 3057 (35) 3057 (34)	3211 (17) 3216 (13) 3217 (21)

Table 3. IR spectroscopy parameters (stretching frequencies and intensities) for free methane and the methane-hydrogen sulphide complex conformers. Calculated values are compared to those from Ref. [38].

The calculated values show a slight red shift in the C-H stretching frequencies upon complex formation, which can be attributed to a weak H-bond formation. Although the calculated values are quite systematically shifted by about -160 cm^{-1} from those reported in Ref. [38], both show the same trends. Again, the main cause of this discrepancy is probably the difference in the basis sets, although the computational method should also have some influence. No general tendencies are observed in the changes of the IR intensities, probably due to the weak nature of the interaction.

The second kind of spectroscopic parameters to be evaluated were the NMR spectroscopy parameters. Variations in chemical shifts and in NQCC are shown in Table 4, whereas SSCC are shown in Table 5.

System	Atom	Variation in chemical shift / ppm	Variation in nuclear quadrupole coupling constant / MHz
$CH_4\cdots SH_2$ (**c1**)	C	0,27	-
	H5	0,42	0
	S	-	0,1
$CH_4\cdots SH_2$ (**c3**)	C	0,52	-
	H5	0,04	0
	H7	0,17	0
	S	-	0,01

Table 4. Variations of calculated NMR spectroscopy parameters upon comlexation for the two methane-hydrogen sulphide complex conformers. Variations in chemical shifts for a nucleus i are calculated as $\Delta\delta_i = \delta_i^{complex} - \delta_i^{free}$ (a positive value for $\Delta\delta_i$ means, thus, a shift downfield of the i resonance). Variations in NQCC are calculated in an analogous way. For chemical shifts, the isotopes ^1H and ^{13}C were considered. For NQCC calculations the isotopes ^2H and ^{33}S were considered.

System	Spin-spin coupling constants / Hz
$CH_4\cdots SH_2$ (**c1**)	$^1J_{C\text{-}H5}$ = 125,89
	$^1J_{S\text{-}H5}$ = 0,12
	$^2J_{C\text{-}S}$ = 0,26
$CH_4\cdots SH_2$ (**c3**)	$^1J_{C\text{-}H5}$ = 125,46 ; $^1J_{C\text{-}H7}$ = 123,70
	$^1J_{S\text{-}H5}$ = 0,46 ; $^1J_{S\text{-}H7}$ = 0,34
	$^2J_{C\text{-}S}$ = 1,58
CH_4	$^1J_{C\text{-}H5}$ = 124,34

Table 5. Calculated SSCC for the two conformers for the methane-hydrogen sulphide complex and free methane. The isotopes ^1H, ^{13}C and ^{33}S were considered.

Typical variations of ^1H chemical shifts upon H-bond formation are in the range of 1 and 4 ppm, whereas for ^{13}C acting as H-donor variations between 4 and 7 ppm are expected [25]. These values refer to medium strength H-bonds. The obtained results are in agreement with the referenced ones in their sign but their magnitude is significantly lower, which highlights the weak nature of the interaction.

For C-H SSCC, being the C atom the H-donor in a H-bond, variations in the range of 2 and 4 Hz are expected [25]. In the studied $CH_4\cdots SH_2$ complex variations of about 1 Hz are observed, which can be interpreted as a consequence of the weak H-bond formation. The presence of an intermolecular C-S spin-spin coupling is indicative of some bonding character in the CH···S contact, that is, that a H-bond exists. However, the small magnitude of this SSCC reflects again its weak character.

NQCC for a given quadrupolar nucleus usually decrease when this nucleus is involved in a H-bond. Typically changes of about 1 to 20 MHz are observed, depending on the nucleus and whether it acts as H-donor or H-acceptor [39]. The calculated changes in the NQCC for ^{33}S do not follow this tendency, and their magnitudes are too small for drawing conclusions from them.

6.1.2.3. Theoretical criteria

In order to confirm H-bonding between methane and hydrogen sulphide, AIM analyses were performed searching for bond critical points (bond cps). The results are shown in Table 6. The graphical representations of the bond cps as well as their associated bond paths are shown in Scheme A1.1 in Appendix 1.

Contact (system)	Critical point (type of cp)	Electron density at the cp ($\rho(\vec{r}_c)$ / $e \cdot a_0^{-3}$)	Hessian of the electron density at the cp ($\nabla^2\rho(\vec{r}_c)$ / $e \cdot a_0^{-5}$)
CH5···S (**c1**)	(3,-1) (bond cp)	5,168·10^{-3}	-3,033·10^{-3}
CH5···S (**c3**)	(3,-1) (bond cp)	3,117·10^{-3}	-2,662·10^{-3}
CH7···S (**c3**)	(3,-1) (bond cp)	3,102·10^{-3}	-2,651·10^{-3}
H5···S···H7(**c3**)	(3,+1) (ring cp)	3,066·10^{-3}	-2,692·10^{-3}

Table 6. AIM analysis data for the two conformers of the methane-hydrogen sulphide complex.

These results are in agreement with a similar study performed by Domagała and Grabowski [40], although they consider it difficult to establish whether the $CH_4\cdots SH_2$ is a H-bond and they opt to classify it as a van der Waals interaction. Parthasarathi and co-workers, however, classify the $CH_4\cdots SH_2$ interaction as a weak H-bond with similar results of an AIM analysis [21].

Using eq. 4 proposed by Rozenberg, estimates to the H-bond strength were calculated from the electron density values obtained from the AIM analyses. The results are shown in Table 7.

Conformer	Estimated H-bond strength / kcal·mol^{-1}
c1 (CH5···S)	0,077
c3 (CH5···S)	0,67
c3 (CH7···S)	0,68

Table 7. Estimated H-bond strength for the different conformers of the CH_4···SH_2 complex from eq. 4.

The estimated values clearly differ from those given in Ref. [38] (see Table 2); however, they can be taken as rough estimates to the magnitude of the H-bond strength.

6.1.3. Adequacy of the computational model

The computational model used in this study gives good approximations to the geometries obtained by Rovira and Novoa with a more demanding computational model. The trend found for IR parameters agree with Rovira and Novoa's results, and the AIM analysis parallels that of Domagała and Grabowski's results.

The calculated NMR shielding constants and scalar couplings point to a weak H-bond, while NQCC do not support this conclusion. However, these parameters show very little changes upon cluster formation, so the results are little conclusive. On the other hand, NMR parameters are difficult to calculate with accuracy and very sensitive to the approximations used in the computational model. A lack of available literature about NMR studies of analogous interactions to be taken as a reference makes it difficult to assess the accuracy of these results.

Although our computational model correctly predicts the stability of both clusters, it fails to give quantitative interaction energies, mainly due to the lack of diffuse functions in the basis set. Nevertheless, the overall description of the H-bond features is well predicted by the chosen computational model at a relatively low computational cost, so it has been applied to the larger systems presented in the following sections.

6.2. EVALUATION OF THE CH···S INTERACTION IN SIMPLIFIED MODELS OF THE DIMER

6.2.1. Designing the simplified molecular models

After assessing the validity of the computational models that will be used in this study, these methods were applied to the study of the CH···S interaction in the dimer (Scheme 2). In a first approach simplified molecular models that presumably reproduce the CH···S interaction are studied. These models are designed following two criteria: (i) the model must contain the

interacting moieties, and (ii) the model should be as simple as possible in order to be easily studied following the approaches described in Section 5.1.

Two different molecular models were studied. In both of them, the moiety containing the S atom was obtained by taking from the monomer only one of the three three-membered condensed rings (see Schemes 5 and 6 in section 6.2.2.), from now on referred to as fragment **1**. The two studied molecular models differ in how the methyl group is reproduced: in the first model, the methyl group is reproduced by methane, whereas in the second model it is also reproduced by fragment **1**. Table 8 summarizes both dimer models.

Dimer model	Fragments	
	Methyl moiety	Sulphur moiety
1-CH_4	CH_4	**1**
(**1**)$_2$	**1**	**1**

Table 8. Models used to reproduce the CH···S contact in the dimer.

The election of both models has a reason. It seemed that the aromatic environment of the S atom would have a significant influence on its electronic properties, so the whole three-membered rings moiety had to be considered. The influence of the aromatic rings on the properties of the methyl group should be smaller since they are not directly bounded together. Moreover, simplifying this moiety to methane avoids including intermolecular interactions aside from CH···S interactions, so it was decided to consider the **1**-CH_4 model first and then study the (**1**)$_2$ model to include the eventual effects of the three-membered ring on the C-H group.

6.2.2. Potential energy surface minima

Both models **1**-CH_4 and (**1**)$_2$ were optimized to determine their PES minima at different levels of KS-DFT theory, considering in each calculation the corrections described in Section 5.2. A first optimization was performed at the RKS-DFT/def2-SVP level, being the resulting geometries reoptimized at the RKS-DFT/def2-TZVP level. The minimum character of both obtained geometries was confirmed by a frequency calculation. The optimized geometries are shown in Schemes 5 and 6, and the corresponding stabilisation energies in Table 9.

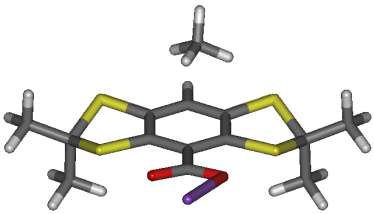

Scheme 5. Equilibrium geometry of **1**-CH_4 optimized at the RKS-DFT/def2-TZVP level.

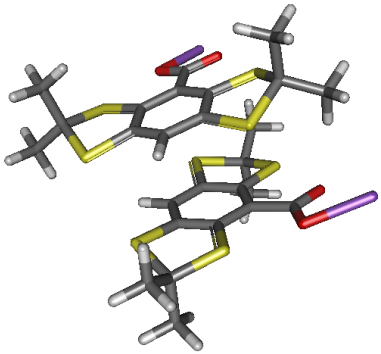

Scheme 6. Equilibrium geometry of $(\mathbf{1})_2$ optimized at the RKS-DFT/def2-TZVP level.

Dimer model	Stabilisation energy / kcal·mol^{-1}
1-CH_4	2,53
$(\mathbf{1})_2$	18,89

Table 9. Stabilisation energies of the dimer models following eq. 2 from the supermolecular approach.

None of the molecular models exhibits the CH···S contact found in the dimer. The **1**-CH_4 model exhibits a large number of energetically close minima in which the methane molecule positions near to the electron-rich aromatic rings, probably stabilized by dispersion forces. In the $(\mathbf{1})_2$ model the two **1** monomers adopt a staggered sandwich-like conformation, with two CH···O contacts between the methyl group of one of the fragments and an O atom from the carboxylate group of the other fragment. In both cases the dimer is more stable than the isolated monomers. The stabilization energy is much larger in the $(\mathbf{1})_2$ model because of the larger number of non-covalent interactions.

No properties other than the equilibrium geometry and the interaction energy were determined for the molecular models since they do not exhibit the CH···S contact interest of this study.

6.3. EVALUATION OF THE CH···S INTERACTION IN THE DIMER

6.3.1. Potential energy surface minima

Both the monomer and the dimer structures were optimized at the UKS-DFT/def2-SVP level. A frequency calculation was carried out to confirm the minimum nature of both optimized structures. Representations of the optimized structures can be found in Schemes 1 and 2 in Section 3.

6.3.2. Calculation of properties

6.3.2.1. Distance and energy criteria

Table 10 shows the interatomic distances between the atoms C, H and S involved in the studied CH···S contact. In the case of the C-H bond length, it is compared to the length of the analogous bond in the monomer.

Contact	Interatomic distance / Å	
	Monomer	Dimer
C-H	1,114	1,112
H···S	–	2,607

Table 10. Some interatomic distances between the atoms C, H and S involved in the CH···S contact.

These values indicate that there might be some change in the nature of the C-H bonding caused by the C-H···S contact, although it should be a weak interaction since variations in the C-H bond length are small. Surprisingly, rather than being larger, the C-H bond is shorter in the dimer than in the monomer. This could mean, if confirmed by other complementary data, that the CH···S contact is an improper H-bond or blue-shifting H-bond.

The first property to be evaluated was the interaction energy of the CH···S contact. This interaction energy was estimated using the rotation barrier approach, that is, from eq. 3. Thus, the rotation barriers of a methyl group in the dimer and in the monomer, that is, a methyl group showing a CH···S contact and a free methyl group, respectively, were calculated. These results as well as the CH···S interaction energy estimated from eq. 3 are shown in Table 11. The

calculated potential energy diagrams associated to the methyl rotations are shown in Schemes A1.2 and A1.3 in Appendix 1.

Compound	Rotation barrier / kcal·mol^{-1}
Monomer	3,97
Dimer	4,21
Estimated H-bond strength / kcal·mol^{-1}	0,24

Table 11. Rotation barriers of a methyl group in the monomer and in the dimer and estimation of the H-bond strength following the rotation barrier approach.

These results show a very weak interaction energy related to the CH···S contact. With this interaction energy, the CH···S contact falls in the range of weak H-bonds in the limit of van der Waals interactions; that is, such a value by itself does not allow to distinguish whether the interaction is caused by dispersion forces or by H-bonding [7,21]. However, it must be recalled that the rotation barrier approach only provides approximate interaction energies. Usually the interaction energies given by the rotation barrier approach are underestimates, since the interacting atoms do not completely move away upon a rotation.

Directionality is one of the criteria recommended by the IUPAC in order to characterize a H-bond. However, this criterion could not be evaluated in this system. The large number of noncovalent interactions present between both monomers in the dimer as well as the closed-packed structure it adopts make it impossible to change structural parameters that would allow to study the dependence of the interaction energy on directionality.

6.3.2.2. Spectroscopic criteria

Both IR spectroscopy and NMR spectroscopy parameters were calculated for the monomer and the dimer in order to assess the H-bond character of the CH···S interaction.

Table 12 shows the IR parameters obtained from a frequency calculation. The corresponding simulated spectra are shown in Schemes A1.4 and A1.5 in Appendix 1, as well as a graphical representation of the normal modes of vibration in Scheme A1.6.

Bond vibration	IR spectroscopy parameters: stretching frequencies / cm^{-1} (intensity $km \cdot mol^{-1}$)	
	Monomer	Dimer
C-H stretching	2918,37 (54,5)	2929,38 (26,2)
	2919,37 (42,8)	2930,09 (35,0)
	2922,93 (33,2)	2932,70 (29,9)

Table 12. IR spectroscopy parameters (stretching frequencies and intensities) for the C-H bond in the monomer and in the dimer.

The calculated data show a clear influence of the molecular association in the C-H stretching modes. However, not a red-shift nor an intensification of the stretching frequencies is observed: the stretching frequencies are blue-shifted and less intense. As suggested by the shortening of the C-H length upon dimer formation, the IR spectroscopy parameters point to a blue-shifting H-bond between the CH···S atoms.

The second kind of spectroscopic parameters to be evaluated were the NMR spectroscopy parameters. Variations in chemical shifts and NQCC are shown in table 13, whereas SSCC are shown in Table 14.

Atom	Variation in chemical shift / ppm	Variation in nuclear quadrupole coupling constant / MHz
C	0,32	-
H	1,53	0,006
S	-	0,24

Table 13. Variations of calculated NMR spectroscopy parameters for the atoms involved in the CH···S contact upon dimer formation. Variations in chemical shifts for an atom i are calculated as $\Delta\delta_i = \delta_i^{dimer} - \delta_i^{monomer}$ (a positive value for $\Delta\delta_i$ means, thus, a shift downfield of the i resonance). Variations in NQCC are calculated in an analogous way. For chemical shifts, the isotopes ^{1}H and ^{13}C were considered. For NQCC calculations the isotopes ^{2}H and ^{33}S were considered.

System	Spin-spin coupling constants / Hz
Dimer	$^{1}J_{C\text{-}H}$ = 17,89
	$^{1}J_{S\text{-}H}$ = -0,61
	$^{2}J_{C\text{-}S}$ = 1,686
Monomer	$^{1}J_{C\text{-}H}$ = 15,76

Table 14. Calculated SSCC for the dimer and the monomer. The isotopes ^{1}H, ^{13}C and ^{33}S were considered.

The results for NMR calculation properties are of the same magnitude than those obtained for the $CH_4 \cdots SH_2$ complex (Section 6.1.2.2). The sign of the variations upon dimer formation indicates a deshielding of the nuclei, which is quite significant for the proton, in agreement with Ref. [25]. The magnitude of this deshielding points again to a weak H-bond.

The observed spin-spin coupling between the C and S atoms from the dimer gives further support to the presence of a H-bond in the CH···S contact, and the increase of the C-H coupling upon dimerization agrees with the blue-shifting character of the bond, and correlates with the observed shortening of the C-H distance. The S-H SSCC is too small to have any clear physical significance.

6.3.2.3. Theoretical criteria

The AIM analysis of the calculated electron density of the dimer confirmed the presence of a H-bond between the CH···S atoms by showing the existence of a bond critical point (a (3,-1) cp) connecting them. The results of the AIM analysis of the electron density are shown in Table 15.

Contact	Critical point (type of cp)	Electron density at the cp ($\rho(r_c) / e \cdot a_0^{-3}$)	Hessian of the electron density at the cp ($\nabla^2\rho(r_c) / e \cdot a_0^{-5}$)
CH···S	(3,-1) (bond cp)	$1{,}496 \cdot 10^{-2}$	$-7{,}548 \cdot 10^{-3}$

Table 15. AIM analysis data for the CH···S contact in the dimer.

The electron density at the bond cp is clearly higher than in the interactions described in the $CH_4 \cdots SH_2$ complex, meaning the CH···S interaction is stronger in the dimer than in the model complex. Taking the value of the electron density at the cp as a reference and comparing it to analogous values reported by Parthasarathi et al. [21], the H-bond strength of the CH···S contact in the dimer is comparable to the H-bond present in $H_2S \cdots H_2S$, $PH_3 \cdots H_2O$ or $PH_3 \cdots HCl$, among others. An estimate to the H-bond strength was obtained using eq. 4. The result is shown in Table 16.

Contact	Estimated H-bond strength / kcal·mol^{-1}
CH···S	2,77

Table 16. Estimated H-bond strength of the CH···S contact in the dimer from eq. 4.

This value is higher than that obtained following the rotation barrier approach. However, both energies –the one obtained by the rotation barrier approach and the one estimated from the electron density at the bond cp– should only be considered in a qualitative way. Both

energies fall in the range of weak H-bonds, that is, a H-bond with little electrostatic contribution and a great dispersion factor.

6.3.3. Evaluation and interpretation of the nature of the CH···S contact

Some of the criteria recommended by the IUPAC on H-bonding have been applied to the assessment of the nature of the CH···S interaction in the dimer. The results obtained from applying these criteria are consistent with each other, leading to the confirmation of a H-bond between the studied atoms. This H-bond clearly falls in the range of weak H-bonds, close to the limit with dispersion forces. Moreover, the CH···S interaction behaves as a "non-conventional" H-bond, that is, a blue-shifting H-bond, as follows from IR and NMR spectroscopic data and from the contraction of the C-H bond length upon H-bond formation.

Joseph and Jemmis consider that X-H bonds, while they are involved in H-bonding, face opposing contracting and lengthening forces [9]. The contracting force is due to the electron affinity of X (the H-donor), which causes a net gain of electron density at the X-H bond region in the presence of Y (the H-acceptor). The lengthening force is due to the well understood attractive interaction between the positively polarized H and the electron rich Y. For electron rich, highly polar X-H bonds, the latter almost dominates the results in X-H elongation, whereas for the less polar, electron poor X-H bonds, the effect of the former is noticeable if Y is not a very strong H-acceptor.

The calculated results seem to agree with the explanation given by Joseph and Jemmis. The almost apolar C-H bond is not as electron rich as other "classical" X-H bonds of groups involved in H-bonding. On the other hand, the H-acceptor is a weak Lewis base that does not pull on the H atom with great force. The studied CH···S interaction is, thus, a weak blue-shifted H-bond, whose physical origin can be attributed mainly to dispersion forces with a very little overlap component.

7. CONCLUSIONS

The CH···S interaction present between a methyl group and a S atom from a cyclic thioether in a dimer was studied in order to assess its possible H-bond character. The study was based on IUPAC's recommendations on the characterization of H-bonding, which include several criteria for characteristic H-bond parameters.

The mentioned criteria were studied following a computational approach. A medium-quality computational model was used, which had to be accurate enough to properly describe weak non-covalent interactions but also not be too computationally demanding, considering the size of the dimer in which the interaction occurs. The validity of the proposed computational model was assessed by first applying the H-bond criteria to a model complex, the $CH_4 \cdots SH_2$ complex, and comparing the results to an analogous study performed by Rovira and Novoa [38]. As a conclusion from this comparative study, it was concluded that the chosen computational model should give correct predictions, although the agreements are only qualitative for the stabilization energies.

The CH···S interaction was then studied in simplified models of the dimer. The results showed that no CH···S contact occurred in these models, probably because the CH···S contact is forced in the dimer by the global conformation it adopts.

The results of applying IUPAC's criteria to the CH···S interaction are consistent with each other, leading to the confirmation of a weak blue-shifted H-bond, whose interaction energy falls in the range of weak H-bonds in the limit of dispersion forces. Also, different approaches (not included in IUPAC's recommendations) were taken to evaluate the interaction energy, namely the rotation barrier approach and the correlation of H-bond strength to the electron density at the H-bond critical point. Nevertheless, the calculated interaction energy depends heavily on the approach taken, and only qualitative conclusions can be drawn from these results.

Not all of the stated objectives could be studied. The magnitude of the variations in the calculated NQCC did not allow making any solid conclusions on their meaning. Also, the directionality of the CH···S interaction (a criterion highlighted by IUPAC's recommendations) could not be assessed.

The proposed classification of the CH···S interaction as a weak H-bond can be taken as accurate, despite the medium-quality computational model used to study it, given the coherence between the different adopted approaches. However, further explorations with higher-quality

models will bring a greater insight into the nature of this interaction. The interaction energy was not well established in this study, and an energetic analysis in terms of the different contributions would reveal more about the physical origin of this interaction. Furthermore, it has been suggested that blue-shifting H-bonds recalculated at higher levels of approximation may be treated as usual red-shifting H-bonds [40]. Thus, the blue-shifting character of the studied interaction should not be taken as the ultimate classification.

8. REFERENCES AND NOTES

1. Maly, T.; Debelouchina, G. T.; Bajaj, V. S.; Hu, K.; Joo, C.; Mak-Jurkauskas, M. L.; Sirigiri, J. R.; van der Wel, P. C. A.; Herzfeld, J.; Temkin, R. J.; Griffin, R. G. Dynamic nuclear polarization at high magnetic fields. *J. Chem. Phys.* **2008**, *128*, 52211.
2. Ardenkjær-Larsen, J. H.; Fridlund, B.; Gram, A.; Hansson, G.; Hansson, L.; Lerche, M. H.; Servin, R.; Thaning, M.; Golman, K. Increase in signal-to-noise ratio of >10000 times in liquid-state NMR. *PNAS*, **2003**, *100 (18)*, 10158-10163.
3. Marín-Montesinos, I.; Paniagua, J. C.; Vilaseca, M.; Urtizberea, A.; Luis, F.; Feliz, M.; Lin, F.; van Doorslaer, S.; Pons, M. Self-assembled trityl radical capsules – implications for dynamic nuclear polarization. *Phys. Chem. Chem. Phys.* **2015**, *17 (8)*, 5785-5794.
4. Latimer, W. M.; Rodebush, W. H. Polarity and ionization from the standpoint of the Lewis Theory of Valence. *J. Am. Chem. Soc.* **1920**, *42*, 1419.
5. Pauling, L. *The Nature of the Chemical Bond*. Cornell University Press: Ithaca, New York, 1939.
6. Arunan, E.; Desiraju, G. R.; Klein, R. A.; Sadlej, J.; Scheiner, S.; Alkorta, I.; Clary, D. C.; Crabtree, R. H.; Dannenberg, J. J.; Hobza, P.; Kjaergaard, H. G.; Legon, A. C.; Mennucci, B.; Nesbitt, D. J. Definition of the hydrogen bond (IUPAC Recommendations 2011). *Pure Appl. Chem.* **2011**, *83 (8)*, 1637-1641.
7. Arunan, E.; Desiraju, G. R.; Klein, R. A.; Sadlej, J.; Scheiner, S.; Alkorta, I.; Clary, D. C.; Crabtree, R. H.; Dannenberg, J. J.; Hobza, P.; Kjaergaard, H. G.; Legon, A. C.; Mennucci, B.; Nesbitt, D. J. Defining the hydrogen bond: an account (IUPAC Technical Report). *Pure Appl. Chem.* **2011**, *83 (8)*, 1619-1636.
8. Buckingham, A. D., in *Intermolecular Interactions from Diatomics to Biopolymers*; Pullman, B., Ed.; John Wiley: New York, 1978.
9. Joseph, J.; Jemmis, E. D. Red-, blue-, or no-shift in hydrogen bonds: a unified explanation. *J. Am. Chem. Soc.* **2007**, *129*, 4620-4632.
10. Iogansen, A. I. Direct proportionality of the hydrogen bonding energy and the intensification of the stretching υ(XH) vibration in infrared spectra. *Spectrochimica Acta Part A*. **1999**, *55*, 1585-1612.
11. Jones, R. O.; Gunnarsson, O. The density functional formalism, its applications and prospects. *Rev. Mod. Phys*. **1989**, *61 (3)*, 689-746.
12. Hohenberg, P.; Kohn, W. Inhomogeneous electron gas. *Phys. Rev.* **1964**, *136 (3B)*, 864-871.
13. Kohn, W. Nobel Lecture: electronic structure of matter – wave functions and density functionals. *Rev. Mod. Phys.* **1999**, *71 (5)*, 1253-1266.
14. Kohn, W.; Sham, L. J. Self-consistent equations including exchange and correlation effects. *Phys. Rev.* **1965**, *140 (4A)*, 1133-1138.
15. Grimme, S. Density functional theory with London dispersion corrections. *WIREs Comput. Mol. Sci.* **2011**, *1*, 211-228.
16. Klimeš, J.; Michaelides, A. Perspective: advances and challenges in treating van der Waals dispersion forces in density functional theory. *J. Chem. Phys.* **2012**, *137*, 120901.
17. Bader, R. F. W. *Atoms in Molecules – A Quantum Theory*. Oxford University Press: Oxford, 1990.
18. Cortés-Guzmán, F.; Bader, R. F. W. Complementarity of QTAIM and MO theory in the study of bonding in donor-acceptor complexes. *Coord. Chem. Rev.* **2005**, *249*, 633-662.
19. Popelier, P. L. A. On the full topology of the Laplacian of the electron density. *Coord. Chem. Rev.* **2000**, *197*, 169-189.

20. Rozenberg, M. The hydrogen bond – practice and QTAIM theory. *RSC Adv.* **2014**, *4*, 26928-26931.
21. Parthasarathi, R.; Subramanian, V.; Sathyamurthy, N. Hydrogen bonding without borders: an Atoms-in-Molecules perspective. *J. Phys. Chem. A*, **2006**, *110*, 3349-3351.
22. Müller-Dethlefs, K.; Hobza, P. Noncovalent interactions: a challenge for experiment and theory. *Chem. Rev.* **2000**, *100*, 143-167.
23. Boys, S. F.; Bernardi, F. The calculation of small molecular interactions by the differences of separate total energies. Some procedures with reduced errors. *Mol. Phys.* **1970**, *19*, 553.
24. Buemi, G. Intramolecular hydrogen bonds. Methodologies and strategies for their strength evaluation. In *Hydrogen Bonding – New Insights*; Grabowski, S., Ed.; Springer: Dordrecht, The Netherlands, 2006; Vol. 3; p51.
25. Pecul, M.; Leszczynski, J.; Sadlej, J. Comprehensive ab initio studies of nuclear magnetic resonance shielding and coupling constants in XH···O hydrogen-bonded complexes of simple organic molecules. *J. Chem. Phys.* **2000**, *112*, 7930-7938.
26. (a) Perdew, J. P.; Wang, Y. Accurate and simple density functional for the electronic exchange energy: generalized gradient approximation. *Phys. Rev. B.* **1986**, *33 (12)*, 8800-8802. (b) Becke, A. D. Density-functional exchange-energy approximation with correct asymptotic behaviour. *Phys. Rev. A.* **1988**, *38 (6)*, 3098-3100.
27. (a) Grimme, S.; Antony, J.; Ehrlich, S.; Krieg, H. A consistent and accurate *ab initio* parametrization of density functional dispersion (DFT-D) for the 94 elements H-Pu. *J. Chem. Phys.* **2010**, *132*, 154104. (b) Grimme, S.; Ehrlich, S.; Goerigk, L. Effect of the damping function in dispersion corrected density functional theory. *J. Comput. Chem.* **2011**, *32*, 1456-1465.
28. Kruse, H.; Grimme, S. A geometrical correction for the inter- and intra-molecular basis set superposition error in Hartree-Fock and density functional theory calculations for large systems. *J. Chem. Phys.* **2012**, *136*, 154101.
29. Sinnecker, S.; Rajendran, A.; Klamt, A.; Diedenhofen, M.; Neese, F. Calculation of solvent shifts on electronic g-tensors with the conductor-like screening model (COSMO) and its self-consistent generalization to real solvents (Direct COSMO-RS). *J. Phys. Chem A.* **2006**, *110*, 2235-2245.
30. Neese, F. The ORCA program system. *Wiley Interdiscip. Rev.: Comput. Mol. Sci.* **2012**, *2*, 73-78.
31. Gaussian 09, Revision D.01, M. J. Frisch, G. W. Trucks, H. B. Schlegel, G. E. Scuseria, M. A. Robb, J. R. Cheeseman, G. Scalmani, V. Barone, B. Mennucci, G. A. Petersson, H. Nakatsuji, M. Caricato, X. Li, H. P. Hratchian, A. F. Izmaylov, J. Bloino, G. Zheng, J. L. Sonnenberg, M. Hada, M. Ehara, K. Toyota, R. Fukuda, J. Hasegawa, M. Ishida, T. Nakajima, Y. Honda, O. Kitao, H. Nakai, T. Vreven, J. A. Montgomery, Jr., J. E. Peralta, F. Ogliaro, M. Bearpark, J. J. Heyd, E. Brothers, K. N. Kudin, V. N. Staroverov, T. Keith, R. Kobayashi, J. Normand, K. Raghavachari, A. Rendell, J. C. Burant, S. S. Iyengar, J. Tomasi, M. Cossi, N. Rega, J. M. Millam, M. Klene, J. E. Knox, J. B. Cross, V. Bakken, C. Adamo, J. Jaramillo, R. Gomperts, R. E. Stratmann, O. Yazyev, A. J. Austin, R. Cammi, C. Pomelli, J. W. Ochterski, R. L. Martin, K. Morokuma, V. G. Zakrzewski, G. A. Voth, P. Salvador, J. J. Dannenberg, S. Dapprich, A. D. Daniels, O. Farkas, J. B. Foresman, J. V. Ortiz, J. Cioslowski, and D. J. Fox, Gaussian, Inc., Wallingford CT, 2013.
32. Allouche, A. R. Gabedit – A graphical user interface for computational chemistry softwares. *J. Comput. Chem.* **2011**, *32*, 174-182.
33. AIMAll (Version 14.11.23), Todd A. Keith, TK Gristmill Software, Overland Park KS, USA, 2014 (aim.tkgristmill.com).
34. Schäfer, A.; Horn, H.; Ahlrichs, R. Fully optimized contracted gaussian basis sets for atoms Li to Kr. *J. Chem. Phys.* **1992**, *97*, 2571.
35. (a) Schindler, M.; Kutzelnigg, W. J. Theory of magnetic susceptibilities and NMR chemical shifts in terms of localized quantities. II. Application to some simple molecules. *J. Chem. Phys.* **1982**, *76*, 1919. (b) Kutzelnigg, W. J.; Fleischer, U.; Schindler, M. *The IGLO Method: Ab Initio Calculation and Interpretation of NMR Chemical Shifts and Magnetic Susceptibilities*. Springer-Verlag: Heidelberg, Germany, 1990.

36. Dykstra, C. E.; Lisy, J. M. Experimental and theoretical challenges in the chemistry of noncovalent intermolecular interaction and clustering. *Journal of Molecular Structure (Theochem).* **2000**, *500*, 375-390.
37. Helgaker, T.; Watson, M.; Handy, N. C. Analytical calculation of nuclear magnetic resonance indirect spin-spin coupling constants at the generalized gradient approximation and hybrid levels of density-functional theory. *J. Chem. Phys.* **2000**, *113*, 9402.
38. Rovira, C.; Novoa, J. J. Strength and directionality of the C(sp^3)-H···S(sp^3) interaction. An ab initio study using the H_2S···CH_4 model complex. *Chemical Physics Letters.* **1997**, *279*, 140-150.
39. Legon, A. C. The nature of ammonium and methylammonium halides in the vapour phase: hydrogen bonding *versus* proton transfer. *Chem. Soc. Rev.* **1993**, *22*, 153-163.
40. Domagała, M.; Grabowski, S. C-H···N and C-H···S hydrogen bonds – influence of hybridization on their strength. *J. Phys. Chem.* **2005**, *109*, 5683-5688.

9. ACRONYMS

AIM: Atoms in Molecules (*see also QTAIM*)

BSSE: Basis set superposition error

BP86: Becke-Perdew '86 exchange correlation functional

cp: critical point

CP method: counterpoise method

DFT: Density functional theory

DNP: Dynamic nuclear polarisation

gCP method: geometrical counterpoise method

H-bond: Hydrogen bond

HF: Hartree-Fock

HK: Hohenberg-Kohn

IR: Infrared

KS: Kohn-Sham

NMR: Nuclear magnetic resonance

NQCC: Nuclear quadrupole coupling constant

PES: Potential energy surface

QTAIM: Quantum theory of Atoms in Molecules

RKS: Restricted Kohn-Sham

ROKS: Restricted open-shell Kohn-Sham

SCF: Self-consistent field

SSCC: Spin-spin coupling constant

UKS: Unrestricted Kohn-Sham

APPENDICES

APPENDIX 1: SELECTED IMAGES

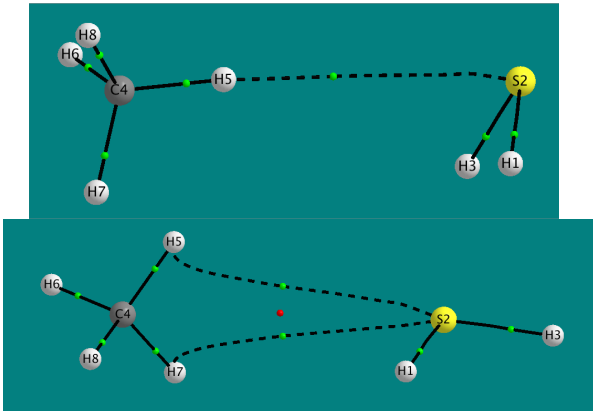

Scheme A1.1. Representation of the different critical points found in the AIM analysis of the electron density of the methane-hydrogen sulphide complex conformers (**c1** is shown top and **c3** is shown down). Bond cps are shown as green dots and ring cps as red dots. Bond paths are shown as solid black lines whereas the H-bond bond paths are shown as dashed black lines.

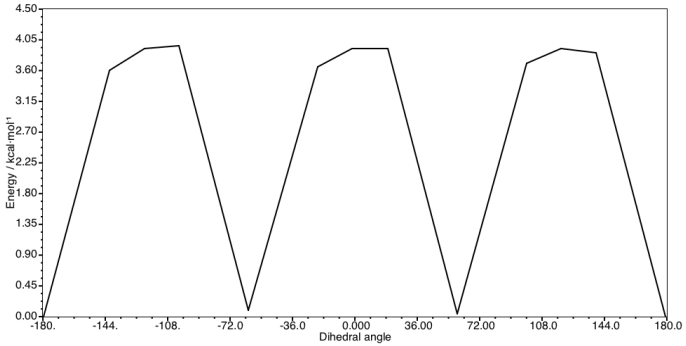

Scheme A1.2. Potential energy diagram for the methyl group rotation in the monomer (free rotation). Relative energies are shown as the rotation angle varies (the values for the angle are meaningless).

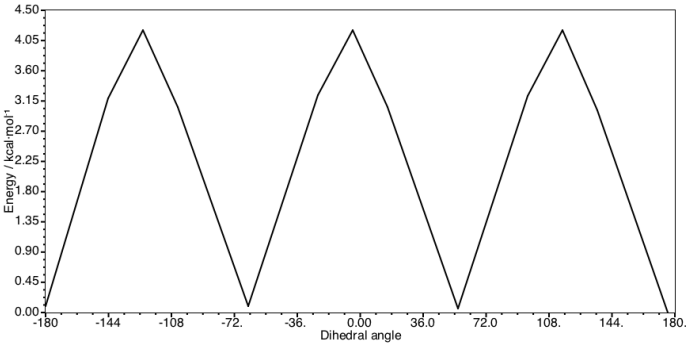

Scheme A1.3. Potential energy diagram for the methyl group rotation in the dimer (rotation with CH···S contact). Relative energies are shown as the rotation angle varies (the values for the angle are meaningless).

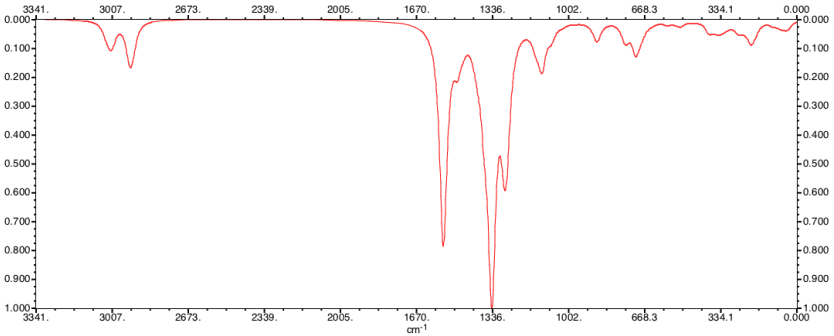

Scheme A1.4. Simulated IR spectrum of the monomer.

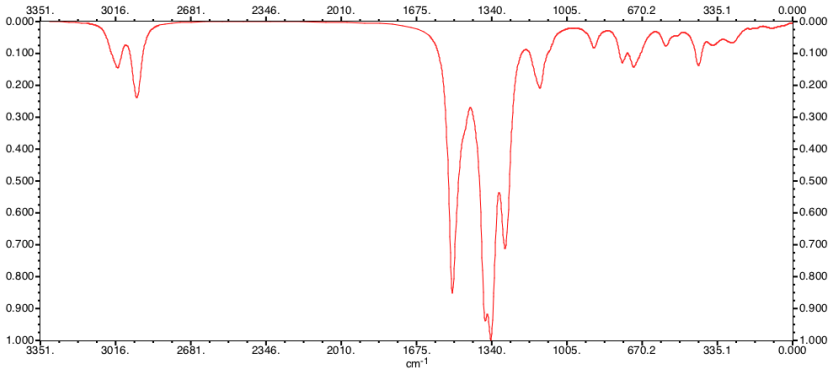

Scheme A1.5. Simulated spectrum of the dimer.

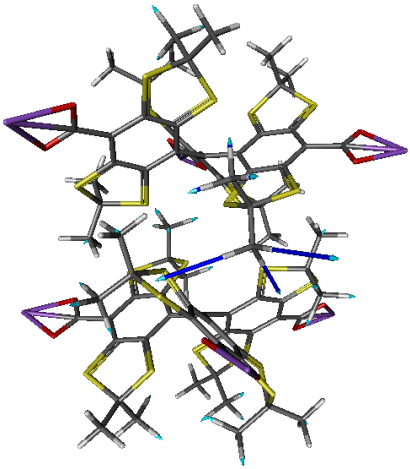

Scheme A1.6. Representation of the vibration corresponding to the C-H stretching of the methyl group involved in the CH···S contact.